Methanol to Gasoline-Range Hydrocarbons: Influence of Nanocrystal Size and Mesoporosity on Catalytic Performance and Product Distribution of ZSM-5

ARTICLE *in* INDUSTRIAL & ENGINEERING CHEMISTRY RESEARCH · SEPTEMBER 2011

Impact Factor: 2.59 · DOI: 10.1021/ie201549j

2 AUTHORS:

Ali Rownaghi
Georgia Institute of Technology
26 PUBLICATIONS **235** CITATIONS
SEE PROFILE

Jonas Hedlund
Luleå University of Technology
140 PUBLICATIONS **2,593** CITATIONS
SEE PROFILE

I&EC research
Industrial & Engineering Chemistry Research

ARTICLE

pubs.acs.org/IECR

Methanol to Gasoline-Range Hydrocarbons: Influence of Nanocrystal Size and Mesoporosity on Catalytic Performance and Product Distribution of ZSM-5

Ali A. Rownaghi* and Jonas Hedlund

Division of Chemical Technology, Luleå University of Technology, SE-971 87 Luleå, Sweden

ABSTRACT: Improvement of synthesis methods for ZSM-5 zeolite, as a heteregeneous catalyst, is essential for a wide variety of different reactions in the chemical industry. Decreasing zeolite crystal size and introducing mesoporosity into the zeolite structure can improve its performance in catalytic reaction through decreasing the micropore diffusion path-length and increasing the external surface area. In this study, three different ZSM-5 zeolites (Nano-ZSM-5, Meso-ZSM-5, and Con-ZSM-5) were prepared by a single-templating procedure, and the reaction of methanol to gasoline-range hydrocarbons was evaluated over synthesized ZSM-5 crystals in a fixed-bed continuous flow reactor. Good correlation was observed between catalytic performance, product distribution, mesoporosity, and crystal size of ZSM-5 zeolites. Both nanocrystal and mesoporous ZSM-5 zeolites showed long-term catalytic stability compared with the conventional one. In contrast to conventional ZSM-5 catalyst, the nanocrystal and mesoporous ZSM-5 catalysts showed high selectivities for light olefins and alkyl aromatics, respectively, in the conversion of methanol to gasoline. These results clearly indicate that both crystal size and mesoporosity significantly influence the ZSM-5 lifetime and product distribution.

1. INTRODUCTION

Methanol-to-gasoline (MTG) reaction is considered one of the widely used technologies for production of high-octane gasoline from biomass, natural gas, and coal.[1−4] With MTG technology, one can make almost any product (i.e., fuels, light olefins or chemicals) out of biomass, natural gas, and coal that can be made out of crude oil.[1−4] Methanol is normally produced from synthesis gas ($CO + H_2$) through gasification of biomass, coal, or steam reforming of natural gas. The obtained methanol is then converted to hydrocarbons (gasoline, olefins, etc.) at temperatures around 400 °C using a zeolitic catalyst. It is known that methanol conversion to hydrocarbons is a series of reaction by which methanol is first dehydrated to dimethyl ether (DME) and water and then DME is converted to light olefins.[2−4] The light olefins thereafter react to form iso- and cycloparaffins and alkyl aromatics. The mechanism of alkyl aromatics formation from methanol is presented as

$$2CH_3OH = \text{dimethyl ether (DME)}$$
$$+ H_2O \rightarrow \text{light olefins (ethylene propylene)}$$
$$+ H_2O \rightarrow \text{iso- and cycloparaffins, alkyl aromatics}$$

ZSM-5 zeolite is known as a solid acid catalyst for efficient conversion of fossil and biomass resources to fuels and chemicals.[5,6] In addition, ZSM-5 has been observed to exhibit excellent catalytic properties in aromatics compounds synthesis, mainly due to its shape-selectivity characterictic. However, the microporous channels present in its structure may in some cases be a major limitation, because mass transport is slow through these narrow channels, especially when reaction is significantly faster than diffusion in the micropores.[7−10] Scaling down of zeolite crystals from micrometer to nanometer scale and developing mesoporous zeolite catalysts have been recognized as important factors in improving processes such as methanol to gasoline and alkylation of benzene with ethene.[11] The mesoporous ZSM-5 in the form of nanosized crystals would display significantly improved characteristics, such as decreased diffusion path length and increased external surface area and catalytic performance, providing easier access to active sites on the external surface and enhanced resistance to coke formation.[7−13]

Recently, several strategies featuring hard-templating and post-treatment (acids or bases leaching) have been proposed for preparing zeolites and other catalysts with certain proportion of mesoporosity.[14−16] Treating zeolite crystals with acids or bases by leaching agent (desilyation and dealumination) can cause a severe change in SiO_2/Al_2O_3 ratio and physicochemical properties of zeolite.[17,18]

Herein, we propose a facile and low-cost route for synthesis of high Al-content ZSM-5 nanocrystals and mesoporous ZSM-5 crystals. Although the roles of zeolite crystal size and mesoporosity have been evaluated in environmental processes[19,20] and various hydrocarbon conversion processes,[21−23] these effects have not been considered in methanol conversion simultaneously. In this contribution, catalyst lifetime and product distribution are accordingly investigated over uniform ZSM-5 nanocrystals, mesoporous ZSM-5 crystals, and conventional ZSM-5 crystals.

2. EXPERIMENTAL SECTION

2.1. Catalyst Preparation. All ZSM-5 zeolites were synthesized hydrothermally from clear colloidal synthesis mixtures. Tetraethylorthosilicate (TEOS, 98%, Aldrich) and aluminum isopropoxide (AIP, Aldrich) were used as Si and Al sources,

Received: May 24, 2011
Accepted: September 19, 2011
Revised: September 4, 2011
Published: September 19, 2011

dx.doi.org/10.1021/ie201549j | *Ind. Eng. Chem. Res.* 2011, 50, 11872–11878

respectively. Concentrated tetrapropylammonium hydroxide (TPAOH, 40 wt % aqueous solution, AppliChem) was used as template. The detailed synthesis descriptions of ZSM-5 samples are as follows.

2.1.1. Synthesis of Uniform ZSM-5 Nanocrystals. Uniform ZSM-5 nanocrystals (Nano-ZSM-5) were synthesized from a clear solution according to the procedure reported by Rownaghi et al.[23] First, all of the required TEOS, about half of the TPAOH, and half of the water were added to a polypropylene bottle, which was then placed on a shaker at room temperature to hydrolyze TEOS and obtain a clear solution. After hydrolysis of TEOS, all $Al(O\text{-}i\text{-}Pr)_3$, NaOH, and water and the other half of the TPAOH were added to a glass beaker and stirred at room temperature until a clear aluminate solution was formed. The clear silicate solution was then added to the clear aluminate solution in a glass beaker with strong stirring. The stirring of the resulting clear solution was continued for about 20−30 min. The molar composition of synthesis mixtures was $3TPAOH{:}0.5Na_2O{:}0.5Al_2O_3{:}25SiO_2{:}1500H_2O{:}100EtOH{:}3PrOH$. In the next step, the clear solution was transferred into a Teflon-lined stainless steel autoclave and crystallized under hydrothermal conditions at 160 °C during 24−30 h. The final white crystals were purified by repeated centrifugation at 15 000 rpm for 30 min, followed by redispersion in water four times. The purified product was thereafter freeze-dried. The obtained crystals were finally calcined at 500 °C in air for 16 h to remove the template molecules. The Si/Al ratio was ∼50 on the basis of elemental analysis. Finally, single crystals of about 110 nm were obtained.

2.1.2. Synthesis of Mesoporous ZSM-5 Crystals. Meso-ZSM-5 was synthesized by using a molar composition of $3TPAOH{:}0.5Na_2O{:}0.5Al_2O_3{:}25SiO_2{:}1500H_2O{:}100EtOH{:}3PrOH$ according to the following procedure. The aluminum isopropoxide was added to an aqueous solution of tetrapropylammonium hydroxide, water, and NaOH. The mixture was stirred at room temperature to obtain a clear solution. Then, the clear aluminate solution was added to tetraethylorthosilicate in the polypropylene bottle. In order to achieve a total hydrolysis of the silicon species, the final solution was placed on a shaker at room temperature to hydrolyze TEOS and obtain a clear solution. Hydrothermal treatment in a Teflon-lined autoclave for 24−30 h at 160 °C yielded white crystals that were further purified by repeated centrifugation at 15 000 rpm for 30 min followed by redispersion in water four times. The purified product was then freeze-dried. The calcined sample was obtained by treatment of as-synthesized material in static air at 500 °C for 16 h. The Si/Al ratio was ∼50 on the basis of elemental analysis. After air drying, mesoporous ZSM-5 crystals as small as 5 nm in the form of mesoporous aggregates of approximately 300 nm in diameter and an average pore diameter of 8 nm were obtained. This structure is very open, giving rise to very large surface areas and pore volumes.

2.1.3. Synthesis of Conventional ZSM-5 Crystals. A conventional ZSM-5 (Con-ZSM-5) zeolite was synthesized following the procedure described elsewhere[24] and is omitted here. The same chemicals and equipments were used in the present work for the preparation and characterization of ZSM-5 catalysts. All samples were treated three times in a 10 wt % NH_4NO_3 solution at 100 °C for 1 h, rinsed, and then calcined in air at 500 °C for 16 h, prior to catalytic experiments.

2.2. Catalyst Characterization. *2.2.1. X-ray Diffraction (XRD).* XRD was performed to determine the bulk crystalline phases of the catalysts using a Siemens diffractometer model D 5000 running in Bragg−Brentano geometry employing Cu Kα (λ = 1.544 39 Å) radiation to generate diffraction patterns from powder crystalline samples at ambient temperature. The spectra were scanned at a rate of 2.0°/min in the range 2θ = 2°−70°.

2.2.2. Surface Area and Porosity. Nitrogen adsorption/desorption isotherms at −196 °C were recorded using a Micromeritics ASAP 2010 instrument. Before the measurements, the samples were heated to 350 °C in a vacuum for at least 12 h. The Brunauer−Emmett−Teller (BET) equation was used to calculate the specific surface area (S_{BET}) using adsorption data at p/p_0 = 0.05−0.25. The mesopore size distribution was derived from the adsorption branch by using the Barrett−Joyner−Halenda (BJH) method. The micropore volume was determined from a *t*-plot.

2.2.3. Scanning Electron Microscope (SEM). SEM images were recorded using a FEI Magellan 400 L instrument. Zeolite crystals were deposited on a silicon wafer by dispersion, and the sample was calcined in air at 500 °C. SEM images were recorded without any coating. The average crystal length was determined by measuring the length of 30 crystals for each sample.

2.2.4. Temperature-Programmed Desorption (TPD). NH_3-TPD measurments were performed to determine the acid strength and the amounts of the acidic sites on the catalyst by using a ThermoFinnigan TPD/R/O 1100 Series instrument. Pretreating of the catalysts was performed by heating them to 773 K in NH_3 flow (101 kPa, 25 cm^3 min^{-1}) and holding catalysts under that flow at 773 K for 1 h before cooling them to ambient temperature.

2.2.5. Inductively Coupled Plasma-Atomic Emission Spectroscopy (ICP-AES). The bulk composition of the crystals was determined using a Perkin-Elmer Emission Spectrometer Model Plasma 1000 inductively coupled plasma-atomic emission spectrometer (ICP-AES).

2.3. Catalytic Activity Measurements. The catalytic measurments were carried out at atmospheric pressure in adjustable nitrogen flow saturated with methanol in a fixed-bed reactor connected to a gas chromatograph (GC). The feed (N_2) was saturated with methanol (99.9%) in a bubble saturator at 30 °C. The structure temperature was maintained by a constant temperature bath. The inlet flow rate was adjusted using a mass flow controller (MFC). The reaction was carried out in a fixed-bed flow reactor containing a standard mass of catalyst (i.e., 0.50 g) at 370 °C and weight hourly space velocity (WHSV) of 2.6 $g\ g^{-1}\ h^{-1}$. For each test, the powder ZSM-5 catalyst was sieved to 250−300 μm, diluted with inert quartz sand, and then loaded in the reactor. The maximum temperature variation along the bed was ±1 °C. The catalyst and sand were mixed in a 1:10 mass ratio. Soda glass beads and quartz glass were used as catalysts beds in the catalytic test. The catalysts were loaded in a tubular reactor with an internal diameter of 17 mm and a total length of 250 mm. Soda glass beads and quartz glass were placed on the top and bottom of the catalysts. A thermocouple was positioned in the center of the catalyst bed in order to monitor the temperature. The catalyst was then pretreated in situ at a heating rate of 5 °C/min under a flow of air (30 mL/min). When the reactor temperature reached 500 °C, it was maintained at that temperature for 4 h. The temperature was then decreased to the reaction temperature in flowing air. To avoid possible condensation of hydrocarbons, the temperature of the effluent line was constantly maintained at 100 °C. An online Varian 3800 gas chromatograph with a flame ionization detector (GC-FID) equipped with a capillary column (CP-Sil PONA CB fused silica WCOT) analyzed the reaction products with hydrogen as carrier gas. The first sampling of the product gas was done 1 h after the reactant feed

started. During a typical run, subsequent samplings and analyses were done with 1 h sampling periods. To simplify the discussion, we defined light olefins as the sum of ethylene and propylene, alkyl aromatics as the sum of C_6-C_{10} aromatics, paraffins as the sum of C_1-C_4 isoparaffins and paraffins, and the other hydrocarbons as the sum of C_5^+ (alkane and alkene).

3. RESULTS AND DISCUSSION

3.1. Catalyst Characterization. Figure 1 represents the XRD patterns for the investigated ZSM-5 catalysts. These patterns display distinct broad diffraction peaks in 8−10° and 20−25° 2θ ranges, all consistent with typical pattern corresponding to the MFI crystal structure.[25] In contrast to Nano-ZSM-5 and Meso-ZSM-5 samples, Con-ZSM-5 displayed a broad visible background, corresponding to the amorphous parts exist in the sample.

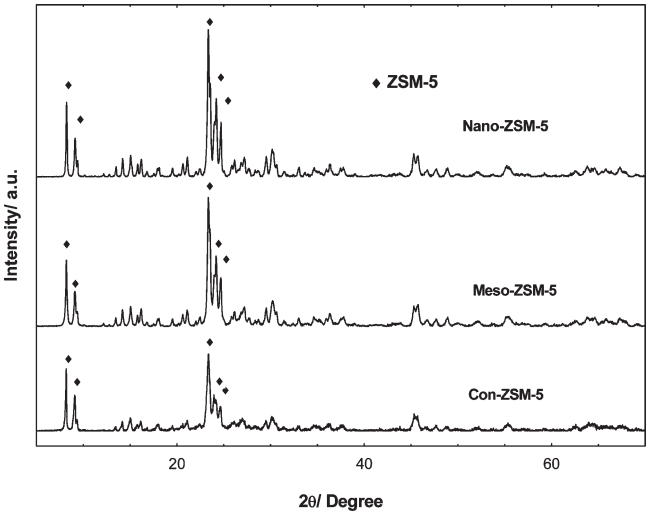

Figure 1. Powder XRD patterns of ZSM-5 zeolites.

The SEM images clearly show the crystal morphology and size of synthesized ZSM-5 zeolites. As shown in Figure 2, the synthesis method significantly influence ZSM-5 morphology and size of the crystals. From each extremely high resolution scanning electron microscope (XHR-SEM) image, approximately 30 ZSM-5 crystals were measured and average values of crystal size were calculated as listed in Table 1. The synthesized samples consist of crystals with different sizes and shapes. Most of these crystals showed typical MFI morphology. Nano-ZSM-5 contains single nanocrystals with hexagonal-cubic morphology, while the shape of Meso-ZSM-5 crystals is roughly ellipsoidal. Meso-ZSM-5 crystals with an average size around 300 nm were formed by aggregates of ultrasmall nanocrystals in the range 5−10 nm. SEM images of Nano-ZSM-5 crystals with very uniform size and morphology confirm the successful synthesis of high-quality ZSM-5 zeolite. In contrast, a large portion of spheroidal crystals exists in Con-ZSM-5 sample, which is mostly made up of platelet-like units. The different morphologies of obtained zeolites were caused to a large extent by synthesis conditions even when the same template was used. Therefore, ZSM-5 zeolites with various sizes and morphologies can be synthesized with the same template by carefully controlling the synthesis conditions. When different synthesis conditions were used, the growth orientation of crystals was different, and thus crystals with different morphologies were produced. For Nano-ZSM-5 sample, a cluster of flaky spheroidal crystals exists on the surface of typical ellipsoidal morphology. This surface morphology could stem from a secondary nucleation yielding smaller crystals. In fact, these crystals deposit onto the primarily formed larger individuals while the outline of their original form was kept. Gabelica et al. reported that in a system where Na^+ is used as a cation, the morphology of synthesized ZSM-5 crystal is more likely to be ellipsoidal−spherical.[26]

ICP-AES analysis of three zeolites indicated that the Si/Al ratios of all samples were almost the same as the synthesis mixtures. The content and strength of acid sites of zeolites were estimated using the NH_3-TPD technique. Figure 3 shows the NH_3-TPD profiles for various ZSM-5 samples. The acidity of

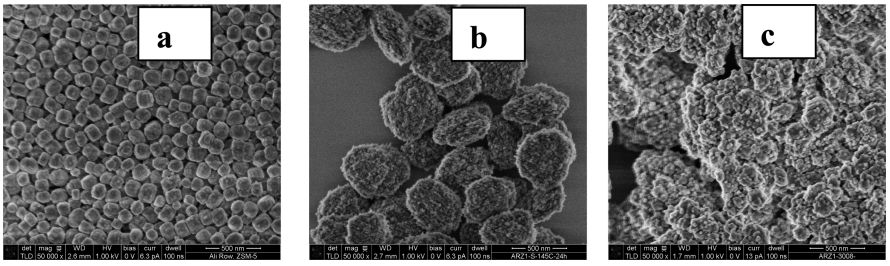

Figure 2. XHR-SEM images of the zeolites: (a) uniform ZSM-5 nanocrystals (Nano-ZSM-5), (b) mesoporous ZSM-5 (Meso-ZSM-5), and (c) conventional ZSM-5 (Con-ZSM-5).

Table 1. Textural Properties of the ZSM-5 Crystals

sample	S_{BET} ($m^2\ g^{-1}$)[a]	S_{meso} ($m^2\ g^{-1}$)[b]	V_{total} ($cm^3\ g^{-1}$)[c]	V_{micro} ($cm^3\ g^{-1}$)[b]	V_{meso} ($cm^3\ g^{-1}$)[d]	D (nm)[e]	crystal size (μm)[f]
Nano-ZSM-5	379	113	0.34	0.08	0.26	3.6	0.12
Meso-ZSM-5	370	138	0.33	0.11	0.22	7.5	0.30
Con-ZSM-5	338	105	0.18	0.11	0.07	3.2	wide-range

[a] Surface areas were obtained by the BET method using adsorption data in the p/p_0 range from 0.05 to 0.25. [b] Measured by the t-plot method. [c] Total pore volumes were estimated from the adsorbed amount at p/p_0 = 0.995. [d] $V_{meso} = V_{ads,p/p_0=99} - V_{micro}$. [e] Average pore diameter were derived from the adsorption branches of the isotherms by using the BJH method. [f] Average particle size are estimated from SEM image.

each peak was calculated from the desorbed amount of NH_3. As can be seen, three peaks were found in NH_3-TPD measurements, leading to the assumption that at least three types of acid sites exist. The first one that appeared in the range 180−250 °C is called the low-temperature peak (α sites) and it is attributed to the desorption of weakly bound ammonia. The concentration of sites was found to be of no catalytic importance,[27] but it is assumed to effectively influence the proton mobility in zeolites, which is an important parameter in gas-sensing applications.[28,29] The second peak, found in the temperature range between 260 and 330 °C, is called the moderate temperature peak (β sites), while the third peak that appeared in the range 340−500 °C is called the high temperature peak (γ sites); these two peaks correspond to ammonia desorption from medium and strong acidic sites, respectively.[26,30] The Con-ZSM-5 catalyst contains three acid sites: α sites generate the peak at 245 °C (weak acid strength), β sites the peak at ∼265 °C (moderate acid strength), and γ sites the peak at ∼420 °C (strong acid strength). In the case of Meso-ZSM-5, two distinct desorption peaks were observed at ∼275 and 460 °C in NH_3-TPD, which are usually ascribed to NH_3 desorption from moderate and strong acid sites. From Con-ZSM-5 to Meso-ZSM-5, it is observed that the β peak shifts to higher temperatures. This shift is accompanied by a gradual increase in the intensity at intermediate temperatures (∼275 °C). The profile of Nano-ZSM-5 shows a single profile at ∼450 °C, which can be quantitatively attributed to the acid site strength. In addition, a shoulder peak at γ sites was observed with a peak maxima at ∼360 °C. The quantitative estimation of acid sites and strength distribution are summarized in Table 2. From the results presented in Table 2, it can be observed that, for all zeolites, the estimated total density values were almost similar, i.e., 0.27, 0.28, and 0.25 mmol/g for Nano-ZSM-5, Meso-ZSM-5, and Con-ZSM-5 catalysts, respectively. In addition, the relative values of total acidities of catalysts are correlated well with the relative amount of aluminum in the bulk catalyst, as estimated by ICP-AES.

The nitrogen adsorption/desorption isotherms of ZSM-5 catalysts were measured at 77 K over calcined samples. The total surface area obtained by the BET equation from adsorption/desorption isotherm data includes contributions from both internal and external surfaces. Total BET surface areas, external surface area (measured by *t*-plot method), total pore volumes (estimated from the adsorbed amount at p/p_0 = 0.995), and average pore diameter were derived from adsorption branches of the isotherms by using the BJH method, and the results are listed in Table 1. As shown in this table, all samples have similar BET surface area as compared with previously reported data.[31,32] The synthesized Nano-ZSM-5 and Meso-ZSM-5 samples display higher BET surface area than Con-ZSM-5 sample, which can be attributed to the higher external and mesopore surface areas of the former catalysts. In line with the results of XHR-SEM (Figure 2) data, some structural differences between these two samples can be deduced. The crystals synthesized by the conventional method show the lowest BET surface area and low crystallinity, which may be assigned to physicochemical properties of the starting materials and the synthesis method.[15,16] In fact, the reason for the lower surface area and crystallinity of Con-ZSM-5 is more likely due to the presence of amorphous units in its structure. To address this problem, an alternative synthesis method was used as reported in our previous studies.[14,23] N_2 sorption data clearly indicate that BET surface area increases as crystal size decreases.

Figure 4 shows different types of N_2 adsorption/desorption isotherms corresponding to the prepared zeolites with Si/Al ratio of 50. Nano-ZSM-5 and Meso-ZSM-5 samples exhibited a type-IV

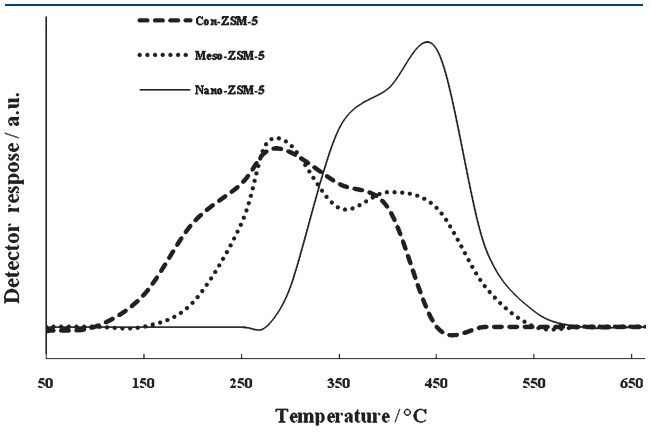

Figure 3. NH_3-TPD patterns of ZSM-5 catalysts.

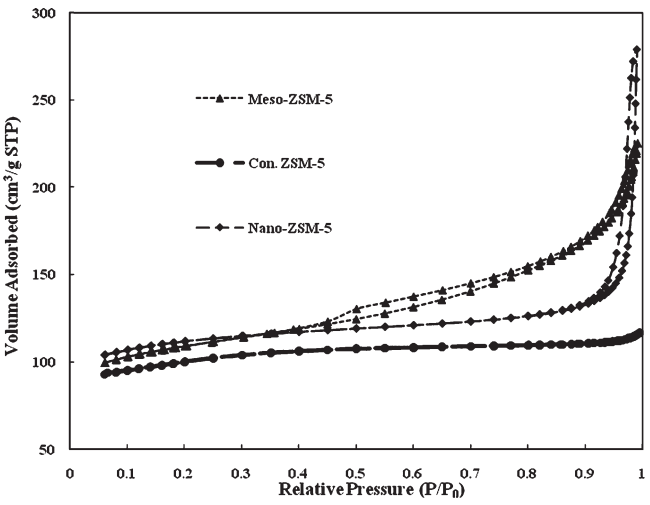

Figure 4. N_2 adsorption/desorption isotherms for ZSM-5 zeolites.

Table 2. Chemical Characterisation of the ZSM-5 Crystals

		number of acid sites (mmol of NH_3/g)[b]						
sample	SiO_2/Al_2O_3 ratios[a]	T_{di} (°C)	weak	T_{di} (°C)	moderate	T_{di} (°C)	strong	total
Nano-ZSM-5	51.1					450	0.27	0.27
Meso-ZSM-5	49.2			275	0.16	460	0.12	0.28
Con-ZSM-5	50.3	245	0.08	265	0.10	420	0.07	0.25

[a] Determined by ICP-AES. [b] Obtained by the NH_3-TPD.

Table 3. Methanol Conversion and Hydrocarbon Distribution (370° C, 1 atm, WHSV = 2.6 g g^{-1} h, methanol partial pressure 0.21 atm, TOS = 10 h)[a]

		average hydrocarbon distribution (wt %)					
catalyst	conversion (%)	ethylene	propylene	paraffins (C_1−C_4)	aromatics (BTX)	other HC	others[b]
Nano-ZSM-5	100	6.6	13.8	33.6	34.2	11.7	0.1
Meso-ZSM-5	70	3.2		7.6	46.9	12.1	0.2
Con-ZSM-5	50	9.6		15.0	18.0	9.6	4.2

[a] Selectivity = (C in product/ΣC converted) × 100. [b] Including CO, CO_2, and coke.

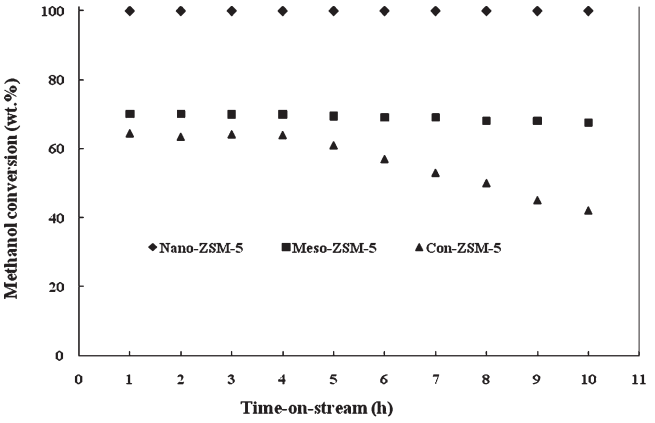

Figure 5. Methanol conversion shows the difference between the Nano-ZSM-5, Meso-ZSM-5, and Con-ZSM-5 zeolites; conversion vs time on stream (370 °C, 1 atm, WHSV = 2.6 g g^{-1} h).

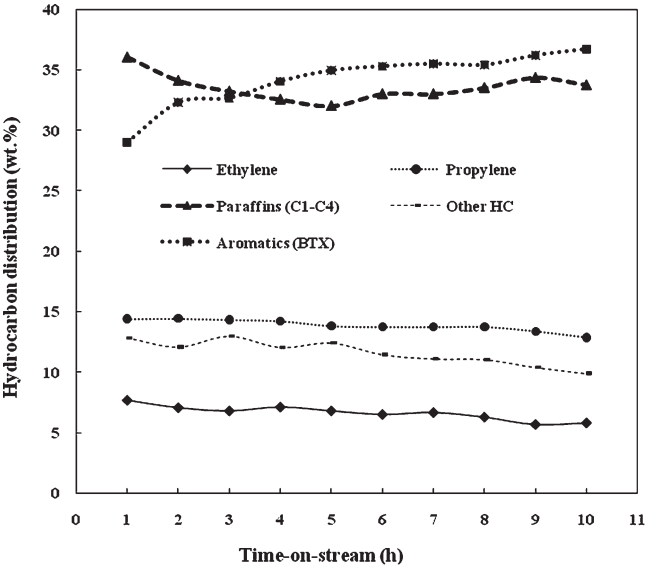

Figure 6. Reaction path for methanol dehydration over uniform ZSM-5 single crystals (Nano-ZSM-5); selectivity vs time on stream (370 °C, 1 atm, WHSV = 2.6 g g^{-1} h).

isotherm,[33] almost similar to that of Con-ZSM-5 sample at low-pressure regions, but with significant increase in adsorption amounts with pressure. Con-ZSM-5 sample, on the other hand, displayed a type-I isotherm (plateau at relative pressure and without hysteresis), which is usually observed for microporous materials having relatively low external surfaces.[33] Characteristic features of type-IV isotherm are basically its hysteresis loop, which is associated with capillary condensation taking place in mesopores, and the limiting uptake over a range of high p/p_0.[33] Nano-ZSM-5 sample showed a type-H_1 loop, which is often associated with porous materials and compacts of approximately uniform spheres in fairly regular array by showing a capillary condensation at relative pressure $p/p_0 = 0.45-0.90$. The capillary condensation was shifted to higher relative pressure of 0.90−0.98 for Nano-ZSM-5 crystals. The Meso-ZSM-5 shows a type-H_4 hysteresis loop, which is often associated with porous materials with narrow slitlike pores. This finding is in accordance with SEM images obtained from the same sample.

The isotherms corresponding to Meso-ZSM-5 and Nano-ZSM-5 crystals indicate that these zeolites are mostly mesoporous, as large amounts of nitrogen adsorption were observed at high p/p_0. Nano-ZSM-5 possesses a total pore volume of 0.3 cm^3 g^{-1} measured at $p/p_0 = 0.995$. It should be pointed out here that the contribution of micrpores to the total pore volume is almost negligible (micropore volume is ∼0.08 cm^3 g^{-1}), providing that this zeolite contains mostly meso- and macrpores in its structure. In fact, the presence of such meso- and macropores in very small crystals of Nano-ZSM-5 zeolite remarkably increases the total pore volume. On the contrary, the total pore volume of Con-ZSM-5 was found to be significantly smaller than that of Nano-ZSM-5 zeolite (0.18 cm^3 g^{-1}). For Meso-ZSM-5, the average pore diameter calculated with the BJH method was 7.5 nm, almost double that of Nano-ZSM-5 (3.6 nm).

3.2. Catalytic Tests: Methanol Dehydration and Hydrocarbons Distribution. Methanol was reacted over 0.5 g of three ZSM-5 catalysts at a temperature of 370 °C and WHSV of 2.6 g g^{-1} h. The catalytic performance and product distribution of uniform mesoporous, nanocrystal, and conventional ZSM-5 catalysts in the dehydration of methanol are listed in Table 3. As data indicate, all samples showed efficient performance in the methanol dehydration reaction. Nano-ZSM-5 catalyst gave rise to the highest activity (100%) during 10 h of operation, which might be attributed to the available number of strong acid sites on the external surface. As pointed out by Paparatto et al.,[34] it is the available number of strong acid sites that plays an influencing role on catalyst activity, not their strength. Compared to Nano-ZSM-5, Meso-ZSM-5 exhibited a lower activity, which reached 70% at the same condition. However, both samples were relatively stable regarding the methanol conversion. On the contrary, Con-ZSM-5 sample showed the lowest activity and stability. The mesoporous and nanocrystalline ZSM-5 zeolites exhibited a significantly higher conversion rate and selectivity toward the desired hydrocarbons than the conventional one, resulting from increased surface area and decreased diffusion path length. Also, both catalysts were more resistant to deactivation occurring due to the coke deposition during reaction. In the case of Con-ZSM-5, since the

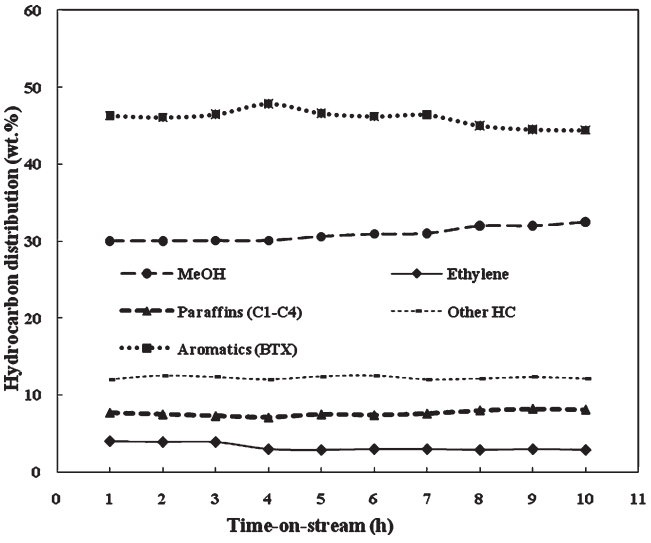

Figure 7. Reaction path for methanol dehydration over mesoporous ZSM-5 nanocrystals (Meso-ZSM-5); selectivity vs time on stream (370 °C, 1 atm, WHSV = 2.6 g g^{-1} h).

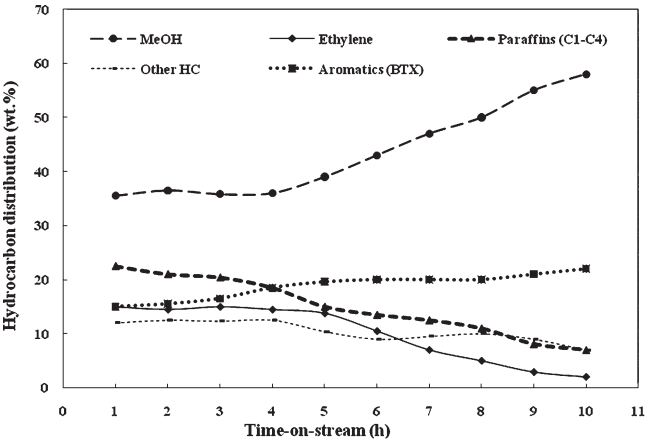

Figure 8. Reaction path for methanol dehydration over conventional ZSM-5 (con-ZSM-5); hydrocarbon distribution vs time on stream (370 °C, 1 atm, WHSV = 2.6 g g^{-1} h).

pore diameter, available number of strong acid sites, and surface area are relatively small, diffusion of products and reactants are relatively slow, resulting in lower conversion.

The higher performance of Nano-ZSM-5 can be attributed to the lower diffusion limitation and higher concentration of strong acid sites on the surface. On the other hand, the slightly lower activity of Meso-ZSM-5 (compared to Nano-ZSM-5) may be partly due to the higher internal concentration of acid sites and diffusional resistance, reducing the overall reaction rate. It has previously been shown[35] that the catalytic activity is proportional to the mesoporosity of catalyst in methanol conversion reaction. However, our obtained results are contrary to this finding. In fact, uniform nanocrystal catalyst (Nano-ZSM-5) shows the highest activity, as a result of easy accessibility of reactants to acid sites. Firoozi et al.[36] had reported that the accessibility and number of strong acid sites on the external surface area instead of acid strength are the major influencing factors on the catalytic conversion of methanol to propylene. Figure 5 confirms that the highly crystalline and uniform Nano-ZSM-5 and Meso-ZSM-5 zeolites display the improved catalytic activity in MTG reaction.

The effects of time on stream on hydrocarbons distribution (i.e., alkane, alkene, and aromatics) and the reaction path on Nano-ZSM-5, Meso-ZSM-5, and Con-ZSM-5 zeolites are shown in Figures 6, 7, and 8, respectively. The product distribution of methanol conversion reaction over all catalysts is also summarized in Table 3. It is important to recall that water is the main product in methanol dehydration reaction, which inhibits methanol dehydration most probably by competitive occupation of acid sites. Furthermore, the observed changes in product distribution can be explained in terms of conversion rate of methanol dehydration. Therefore, water has no direct influence on product distribution. Compared with Meso-ZSM-5 sample, Nano-ZSM-5 catalyst exhibits a relatively low selectivity for alkyl aromatics (BTX) and heavier hydrocarbons and a high selectivity for the formation of light gaseous olefins (ethylene and propylene) and paraffins (C_1-C_4). The contribution of strong acid sites on the external surface of Nano-ZSM-5 is significantly responsible for fewer shape-selective products. The presence of alkane, alkene, and alkyl aromatics in the product stream shows that severe hydrogen transfer occurred in the methanol dehydration reaction. As expected, Meso-ZSM-5 gave higher yields of alkyl aromatics and paraffins and fewer light olefins. This is probably due to the channel structure of mesoporos ZSM-5 crystals.[35] In Meso-ZSM-5, mesopores provide easier access to the active sites in micropores, while micropores provide size and shape selectivity for reactants. The catalytic test results indicate that Meso-ZSM-5 exhibited a significant improvement of catalytic activity and selectivity over conventional ZSM-5 catalyst in methanol-to-gasoline conversion. Figure 8 shows significant reduction in methanol conversion and hydrocarbon selectivity due to the coke formation resulting from decreased surface area and the number of strong acid sites and increased diffusion path length.

Several explanations of these results are possible; one interpretation could be that ethylene and propylene, which are necessary for alkyl aromatics formation, are being hydrogenated to ethane, propane, and higher paraffins. Light olefins (ethylene and propylene) can undergo a variety of reactions such as alkylation with oligomerization, oxygenation, cracking, etc. The general observations for MTG reaction over three ZSM-5 zeolites are as follows:

(1) The conversion of methanol was 100%, 70%, and 50% for Nano-ZSM-5, Meso-ZSM-5, and Con-ZSM-5, respectively.
(2) The gas phase contained large amounts of light olefins and paraffins (C_1-C_4) with a corresponding decrease in aromatics yield over Nano-ZSM-5 zeolite. The aqueous phase consisted of water only.
(3) The liquid gasoline phase consisted of alkyl aromatics, primarily straight and branched aliphatics (C^{5+}) over Meso-ZSM-5. The aqueous phase consisted of water and methanol.

4. CONCLUSION

ZSM-5 catalysts with varied crystal size, mesoporosity, and morphology were synthesized from different synthesis mixtures with the same hydrothermal method. Two different ZSM-5 zeolites (i.e., uniform ZSM-5 nanocrystals and mesoporous ZSM-5) were easily obtained with single step synthesis. The obtained ZSM-5 zeolites consisted of crystals in the range of 100−300 nm. The size of individual crystals, external surface area, and pore size

can be easily controlled by adjusting the preparation of clear synthesis mixure. The combination of physical characteristics such as very small crystal size, high external surface area, and strong acidity makes uniform ZSM-5 nanocrystals a potentially interesting catalyst in processes with severe diffusional limitations for conversion and cracking of bulky molecules. Both Nano-ZSM-5 and Meso-ZSM-5 zeolites exhibited improved catalytic behavior in the methanol conversion reaction. Comparison of catalysts performance indicated that uniform ZSM-5 nanocrystals lead to larger conversion capacity and higher selectivity to light olefins, while a higher yield of alkyl aromatics is obtained over mesoporous ZSM-5 crystals.

AUTHOR INFORMATION

Corresponding Author

*E-mail: ali.rownaghi@gmail.com, ali.rownaghi@ltu.se. Tel: +46 920 49 12 97. Fax: +46 920 49 11 99.

ACKNOWLEDGMENT

The Swedish Energy Agency and the Knut and Alice Wallenberg Foundation are acknowledged for financially supporting the Magellan SEM instrument.

REFERENCES

(1) Gujar, A. C.; Guda, V. K.; Nolan, M.; Yan, Q.; Toghiani, H.; White, M. G. Reactions of methanol and higher alcohols over H-ZSM-5. *Appl. Catal. A: Gen.* **2009**, *363*, 115–121.

(2) Chang, C. D.; Silvestrl, A. J. The conversion of methanol and other O-compounds to hydrocarbons over zeolite catalysts. *J. Catal.* **1977**, *47*, 249–250.

(3) Keil, F. J. Methanol-to-hydrocarbons: Process technology. *Microporous Mesoporous Mater.* **1999**, *29*, 49–66.

(4) Stocker, M. Methanol-to-hydrocarbons: Catalytic materials and their behavior. *Microporous Mesoporous Mater.* **1999**, *29*, 3–48.

(5) Yilmaz, B.; Muller, U. Catalytic applications of zeolites in chemical industry. *Top Catal.* **2009**, *52*, 888–895.

(6) Taarning, E.; Osmundsen, C. M.; Yang, X.; Voss, B.; Andersena, S. I.; Christensen, C. H. Zeolite-catalyzed biomass conversion to fuels and chemicals. *Energy Environ. Sci.* **2011**, *4*, 793–804.

(7) Donk, S.; Janssen, A. H.; Bitter, J. H.; Jong, K. P. Generation, characterization, and impact of mesopores in zeolite catalysts. *Catal. Rev. Sci. Eng.* **2003**, *45*, 297–319.

(8) Rezaei, F.; Webley, P. Structured adsorbents in gas separation processes. *Sep. Purif. Technol.* **2010**, *70*, 243–256.

(9) Egeblad, K.; Christensen, C. H.; Kustova, M.; Christensen, C. H. Templating mesoporous zeolites. *Chem. Mater.* **2008**, *20*, 946–960.

(10) Groen, J. C.; Peffer, L. A. A.; Moulijn, J. A.; Pérez-Ramírez, J. Mesoporosity development in ZSM-5 zeolite upon optimized desilication conditions in alkaline medium. *Colloids Surf. A* **2004**, *241*, 53–58.

(11) Tao, Y. S.; Kanoh, H.; Kaneko, K. ZSM-5 monolith of uniform mesoporous channels. *J. Am. Chem. Soc.* **2003**, *125*, 6044–6045.

(12) Petushkov, A.; Yoon, S.; Larsen, S. C. Synthesis of hierarchical nanocrystalline ZSM-5 with controlled particle size and mesoporosity. *Microporous Mesoporous Mater.* **2011**, *137*, 92–100.

(13) Hoang, T. Q.; Zhu, Z.; lobban, L. L.; Resasco, D. E.; Mallinson, R. G. Effects of HZSM-5 crystallite size on stability and alkyl-aromatics product distribution from conversion of propanal. *Catal. Commun.* **2010**, *11*, 977–981.

(14) Rownaghi, A. A.; Taufiq-Yap, Y. H.; Rezaei, F. Innovative process for the synthesis of vanadyl pyrophosphate as a hightly selective catalyst for butane oxidation. *Chem. Eng. J.* **2010**, *165*, 328–335.

(15) Tosheva, L.; Valtchev, V. P. Nanozeolites: Synthesis, crystallization mechanism, and applications. *Chem. Mater.* **2005**, *17*, 2494–2513.

(16) Cundy, C. S.; Cox, P. A. The hydrothermal synthesis of zeolites: Precursors, intermediates and reaction mechanism. *Microporous Mesoporous Mater.* **2005**, *82*, 1–78.

(17) Caicedo-Realpe, R.; Perez-Ramirez, J. Mesoporous ZSM-5 zeolites prepared by a two-step route comprising sodium aluminate and acid treatments. *Microporous Mesoporous Mater.* **2010**, *128*, 91–100.

(18) Ogura, M. Towards realization of a micro- and mesoporous composite silicate catalyst. *Catal. Surv. Asia* **2008**, *12*, 16–27.

(19) Kustova, M.Yu.; Rasmussen, S. B.; Kustov, A. L.; Christensen, C. H. Direct NO decomposition over conventional and mesoporous Cu-ZSM-5 and Cu-ZSM-11 catalysts: Improved performance with hierarchical zeolites. *Appl. Catal. B* **2006**, *67*, 60–67.

(20) Melian-Cabrera, I.; Espinosa, S.; Groen, J. C.; Linden, B.; Kapteijn, F.; Moulijn, J. A. Utilizing full-exchange capacity of zeolites by alkaline leaching: Preparation of Fe-ZSM5 and application in N_2O decomposition. *J. Catal.* **2006**, *238*, 250–259.

(21) Christensen, C. H.; Schmidt, I.; Christensen, C. H. Improved performance of mesoporous zeolite single crystals in catalytic cracking and isomerization of *n*-hexadecane. *Catal. Commun.* **2004**, *5*, 543–546.

(22) Schmidt, I.; Christensen, C. H.; Hasselriis, P.; Kustova, M.Yu.; Brorson, M.; Dahl, S.; Johannsen, K.; Christensen, C. H. Mesoporous zeolite single crystals for catalytic hydrocarbon conversion. *Stud. Surf. Sci. Catal.* **2005**, *158*, 1247–1254.

(23) Rownaghi, A. A.; Rezaei, F.; Hedlund, J. Yield of gasoline-range hydrocarbons as a function of uniform ZSM-5 crystal size. *Catal. Comm.* **2011**, *14*, 37–41.

(24) Hedlund, J.; Öhrmana, O.; Msimang, L. V.; Steenb, E. V.; Böhringer, W.; Sibya, S.; Möller, K. The synthesis and testing of thin film ZSM-5 catalysts. *Chem. Eng. Sci.* **2004**, *59*, 2647–2657.

(25) Baerlocher, Ch.; McCusker, L. B.; Olson, D. H. *Atlas of Zeolite Framework Types*; Elsevier: New York, 2007.

(26) Gabelica, Z.; Blom, N.; Derouane, E. G. Synthesis and characterization of ZSM-5 type zeolites III. A critical evaluation of the role of alkali and ammonium cations. *Appl. Catal.* **1983**, *5*, 227–248.

(27) Franke, M. E.; Simon, U. Solvate-supported proton transport in zeolites. *Chem. Phys. Chem.* **2004**, *5*, 465–472.

(28) Katada, N.; Igi, H.; Kim, J.; Niwa, M. Synthesis of aniline from phenol and ammonia over zeolite beta. *J. Phys. Chem. B* **1997**, *110*, 5969–5977.

(29) Niwa, M.; Katada, N. Measurements of acidic property of zeolites by temperature programmed desorption of ammonia. *Catal. Surv. Jpn.* **1997**, *1*, 215–226.

(30) Franke, M. E.; Sierka, M.; Simon, U.; Sauer, J. Translational proton motion in zeolite H-ZSM-5. Energy barriers and jump rates from DFT calculations. *Phys. Chem. Chem. Phys.* **2002**, *4*, 5207–5216.

(31) Shirazi, L.; Jamshidi, E.; Ghasemi, M. R. The effect of Si/Al ratio of ZSM-5 zeolite on its morphology, acidity and crystal size. *Cryst. Res. Technol.* **2008**, *43*, 1300.

(32) Kulkarni, S. J.; Srinivasu, P.; Narender, N.; Raghavan, K. V. Fast and efficient synthesis of ZSM-5 under high pressure. *Catal. Comm.* **2002**, *3*, 113–117.

(33) Sing, K. S. W.; Everett, D. H.; Haul, R. A. W.; Moscou, L.; Pierotti, R. A.; Rouquerol, J.; Siemieniewska, T. Reporting physisorption data for gas/solid systems with special reference to the determination of surface area and porosity. *Pure Appl. Chem.* **1985**, *57*, 603–619.

(34) Paparatto, G.; Moretti, E.; Leofanti, G.; Gatti, F. Toluene ethylation on ZSM-5 zeolites. *J. Catal.* **1987**, *105*, 227–232.

(35) Jacobsen, C. J. H.; Madsen, C.; Houzvicka, J.; Schmidt, I.; Carlsson, A. Mesoporous Zeolite Single Crystals. *J. Am. Chem. Soc.* **2000**, *122*, 7116–7117.

(36) Firoozi, M.; Baghalha, M.; Asadi, M. The effect of micro and nano particle sizes of H-ZSM-5 on the selectivity of MTP reaction. *Catal. Commun.* **2009**, *10*, 1582–1585.